Periodic-Error-Free All-Fiber Distance Measurement Method With Photonic Microwave Modulation Toward On-Chip-Based Devices

Yoon-Soo Jang, Jungjae Park, and Jonghan Jin

***Abstract*— High-accuracy distance measurements with compact configurations and robust operations are necessary in areas ranging from precision engineering to scientific missions. Here, we report a precise and accurate amplitude-modulation-based all-fiber distance measurement method without periodic errors. To realize an all-fiber configuration toward on-chip devices in the future, certain selective components for easy fabrication on the chip scale were employed. Despite this constraint, sub-100 nm precision was demonstrated with the help of the all-photonic microwave mixing technique introduced in our previous work. In this article, accuracy as another important factor for measuring distances was investigated to ensure better performance than in previous studies with an optical amplitude-modulation technique. By performing theoretical and experimental analyses of the periodic error while blocking electrical crosstalk signals and optimizing signal processing, accuracy of 2.6 μm (1 σ) was achieved in terms of measurement linearity according to a comparison with a laser displacement interferometer. With the best capabilities of precision and accuracy, the proposed all-fiber distance measurement method is expected to be utilized in diverse long-distance applications, such as large-machine axis tool work and formation flying by multiple satellites. Further, this study demonstrates the possibility of developing an on-chip-based distance-measuring device for the fourth industrial revolution.**

***Index Terms*— Absolute distance measurement, amplitude modulated continuous wave (AMCW) light detection and ranging (LIDAR), microwave photonics, periodic error, photonic microwave mixing.**

I. Introduction

PHOTONIC-BASED microwave frequency mixing is a well-established technique to down-convert high-frequency signals in the field of optical communications [1]. During photonic-based microwave frequency mixing in this application, precision control or monitoring of the phase of the down-converted signal has yet to be studied, as a rough estimation of the phase is sufficient for an analysis of optical communication signals [2], [3]. However, it has started to be considered for dimensional metrology due to the stability and simplicity of the photonics-based microwave frequency mixing technique [4].

In dimensional metrology, a laser displacement interferometer is a representative method to the precise length measurements [5]. However, due to the 2π ambiguity problem, displacements below one-half of the wavelength in use should be continuously sampled and accumulated to determine the length during the entire measurement process. Such an intrinsic limitation means that the laser interferometer cannot be widely exploited for newly emerging applications, especially for long distances. As a counterpart to laser displacement interferometry, absolute distance measurements have been proposed and realized by various approaches [6], [7], including the time-of-flight method [8], [9], amplitude modulation ranging [10]–[14], frequency modulation ranging [15]–[17], spectral resolved interferometry [18]–[20], multi-wavelength interferometry [21]–[23], dual-comb ranging [24]–[26], and microcomb ranging [27]–[29]. One of these examples is light detection and ranging (LIDAR), which works with the time-of-flight method [30].

Given the recent advent of smart factories, autonomous vehicles, outer-space missions, and on-machine metrology, compact sensors capable of determining absolute distances at sub-micrometer precision level are expected to be necessary. To meet this need, the authors reported a 50-nm precision all-fiber absolute distance measuring method [4]. The method was proposed and realized for compact absolute distance measurements based on the amplitude-modulation technique due to its compactness and the simplicity of the system layout. Moreover, with consideration of commercialized fabrication techniques for an on-chip device, only optical fiber components realized by the complementary metal–oxide–semiconductor (CMOS) process were carefully selected. When processing high-frequency microwave signals, the well-known method of photonics-based microwave frequency mixing was adopted as it is known to be immune to the phase conversion amplitude, which otherwise may cause considerable errors. Most amplitude-modulated distance measuring methods are intended to work with electronics-based microwave frequency mixing, which can cause major positioning errors [31]. Despite all of these efforts, photonics-based microwave frequency mixing can cause systematic errors, though this was not studied at that time.

Manuscript received December 1, 2021; accepted January 2, 2022. Date of publication February 4, 2022; date of current version February 24, 2022. This work was supported by the Korea Research Institute of Standards and Science under Grant 22011042 and Grant 22011230. The Associate Editor coordinating the review process was Dr. Yan Zhuang. *(Corresponding author: Jonghan Jin.)*

Yoon-Soo Jang is with the Division of Physical Metrology, Length Standard Group, Korea Research Institute of Standards and Science, Daejeon 305-340, South Korea.

Jungjae Park and Jonghan Jin are with the Division of Physical Metrology, Length Standard Group, Korea Research Institute of Standards and Science, Daejeon 305-340, South Korea, and also with the Department of Science of Measurement, University of Science and Technology, Daejeon 305-350, South Korea (e-mail: jonghan@kriss.re.kr).

Digital Object Identifier 10.1109/TIM.2022.3146896

This work is licensed under a Creative Commons Attribution 4.0 License. For more information, see https://creativecommons.org/licenses/by/4.0/

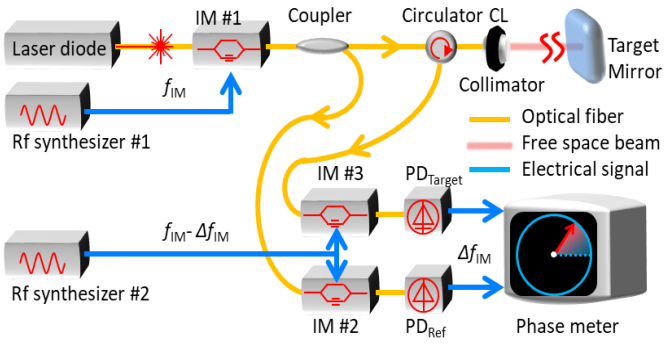

Fig. 1. Configuration of intensity modulation-based distance measurement. IM: intensity modulator, PD: photodiode.

In this article, we investigate the systematic error associated with a method proposed in our previous work. To do that, we have conducted a linearity test compared with a laser displacement interferometry. First, when measuring the displacement, the amount of systematic error that occurs should be assessed. The systematic error typically appears as a periodic pattern. Second, the causes of the systematic error are estimated and verified by a mathematical model. In this case, we observed linearity error of 2.6 μm (1 σ) over 27 mm (2.7 times the ambiguity range), and a periodic pattern was not observed without a post-process. We then artificially create unmeasurable small electrical crosstalk to observe the periodic error, which is a bottleneck in the linearity measurement process. We observed periodic error of ± 20 μm under artificial conditions. We numerically simulated the correlation between the periodic error and the electrical crosstalk and revealed that this level of periodic error can arise due to a small amount of electrical crosstalk of -54 dB. Given its capability of high precision and accuracy during distance measurements and its simple configuration, we believe that the proposed method can be used in calibration of electronic distance measurement (EDM) and will be a powerful candidate for use in conjunction with high-precision chip-scale distance sensors in the future.

II. AMCW-Based Distance Measurements by Means of All-Fiber Photonic Microwave Mixing

The target distance is basically determined by the phase delay (θ) between two amplitude-modulated signals from reference and measurement paths. The amplitude frequency (f_{IM}) determines the ambiguity range ($L_{\mathrm{NAR}} = c/2n_{\mathrm{air}}f_{\mathrm{IM}}$), where c is the speed of light in a vacuum and n_{air} is the refractive index of air. Note that the refractive index of air is assumed as a constant during the measurement, as its variation is low enough to be ignored [29]. The target distance (L) is simply determined by the relationship $L = (M + \theta/2\pi) \times L_{\mathrm{NAR}}$, where M is an integer number.

Fig. 1 describes the optical layout of the all-fiber photonic microwave modulation-based absolute distance measurement. All systems except for the free space path to be measured consisted of fiber components. A fiber laser diode (FRL15DCWB-A81-19580, Furukawa Electric) at a center wavelength of 1.53 μm with optical power of 10 mW was used as a light source in this study. It was modulated by an intensity modulator (LN05S-FC, Thorlabs) (IM #1) driven at 15 GHz, corresponding to an ambiguity distance of 9.993 mm. A microwave synthesizer (SynthHD PRO, Windfreak Technologies, LLC) to drive the intensity modulator was referenced to a cesium atomic clock with a frequency uncertainty of 10^{-13}, [30] which gave direct traceability to a length standard. The modulated beam was divided into the reference and measurement beams by a fiber coupler with a 9:1 split ratio. The reference beam, which was 10% of the modulated beam, goes directly to a secondary intensity modulator (IM#2) for down-conversion of the microwave frequency. The measurement beam, which was 90% of the modulated beam, was initially sent to a target mirror. The reflected beam from the target mirror is directed to an optical circulator and then to another secondary modulator (IM#3) for down-conversion of the microwave frequency. These secondary modulators were driven at 14.99991 GHz ($f_{\mathrm{IM}} - \Delta f_{\mathrm{IM}}$) and both the frequency of the reference and the measurement signals were down-converted to 90 kHz (Δf_{IM}), where the phase delay (θ) can be precisely measured. Additionally, 15 GHz modulated signals were down-converted to 90 kHz, while the phase information was maintained. These down-converted signals were detected by photodiodes. Note that photodiodes do not necessarily have to be high-speed photodiodes. We used photodiodes with a bandwidth of 300 kHz. The phase delay between the reference and measurement signal was measured by a phase meter (Moku: Laboratory, Liquid Instruments) with a sampling rate of 488 Hz to determine the absolute value of the target distance. A target distance beyond the ambiguity range can be determined by a frequency sweeping method [4].

III. Experimental Results of the All-Fiber AMCW Absolute Distance Measurement Method

A. All-Fiber Photonic Microwave Conversion

Fig. 2 describes the all-fiber photonic-based microwave frequency conversion method, which has the advantages of wide frequency coverage, low conversion loss, and immunity to electromagnetic interference compared to an electronic microwave mixer [1]. Cascaded intensity modulators were used for microwave frequency down-conversion, as shown in Fig. 2(a). High-frequency radio frequency (RF) modulated by the intensity modulator (IM#1) was directed to secondary intensity modulators (IM#2 and 3) modulated at a lower frequency which acted as a local oscillator (LO). After secondary intensity modulation (IM#2 and 3), low-frequency intermediated-frequency (IF) signals were generated while the phase delay was maintained. This type of all-photonic-based frequency down-conversion is a powerful tool for frequency down-conversion of microwaves and can replace an electronic microwave mixer in for many applications. It is functionally identical to an electronic microwave mixer. However, microwave components operating at high frequencies are sensitive to the environmental conditions of the input

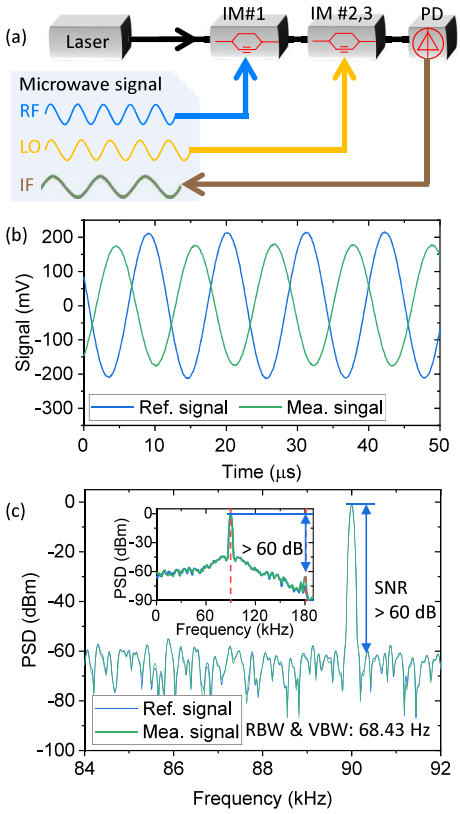

Fig. 2. (a) Simplified configuration of all-fiber microwave down conversion. (b) Time domain signals of reference and measurement signal over 50 μs. (c) PSD of down-converted microwave signal from 84 to 92 kHz. Both reference and measurement signals show >60 dB signal to noise ratio. Inset shows the PSD for broad range.

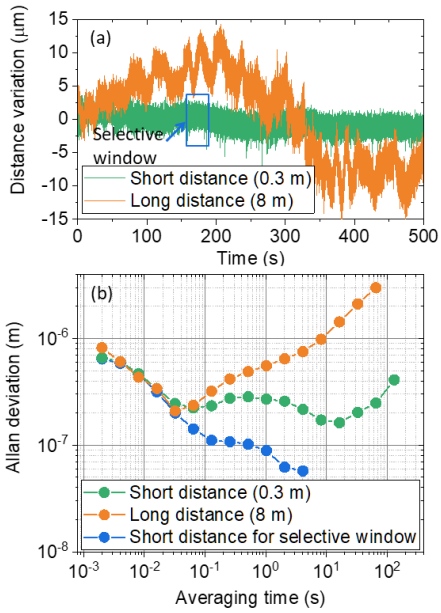

Fig. 3. Typical repeatability by measuring fixed target. (a) Time-dependent variation of the measured distance for short distance (0.3 m) and long distance (8 m). (b) Their Allan deviation from 2 ms to 100 s. Note that blue curves denote the repeatability of selective window for 50 s.

signal [32], [34]. To overcome this limitation of an electronic microwave mixer, we utilized all-photonic microwave frequency conversion instead of an electronic microwave mixer.

The amplitudes of both the reference and measurement signal were adjusted to be nearly identical by an adjustment of the bias voltage of the individual intensity modulators, as shown in Fig. 2(b). In the time domain, clear sinusoidal waveforms with amplitudes exceeding 150 mV for both the reference and measurement signals with a phase delay were observed, as shown in Fig. 2(b). A dual-channel microwave spectrum analyzer (Moku: Lab, Liquid Instruments) was used to measure and monitor simultaneously the power spectral density (PSD) of the down-converted microwave signals. As shown in Fig. 2(c), both signal-to-noise ratios (SNR) of the reference and measurement signals exceeded 60 dB when the resolution bandwidth (RBW) and video bandwidth (VBW) were 68.43 Hz. From dc to 200 kHz with the RBW and VBW were both 1.96 kHz, both the reference signal and measurement signal were 60 dB larger than their second harmonic components, as shown in the inset of Fig. 2(c). This all-photonics-based frequency down-conversion technique has many advantages when applied to amplitude-modulation-based distance measurements. First, it is immune to the amplitude-to-phase conversion process, as demonstrated in our previous study [4]. Second, it does not require a high-speed photodiode. Third, it has high conversion efficiency comparable to that of an electronic microwave mixer.

B. Evaluation of the All-Fiber Photonic-Based Amplitude Modulation Distance Measurement Method

The measurement repeatability was evaluated by measuring fixed distances of about 0.3 m (short distance) and 8 m (long distance). Note that the distance of 8 m relied on the use of a fiber spool. In fact, sub-100 nm measurement repeatability was reported in earlier work ([4]) by the authors together with primary measurement results.

Fig. 3(a) shows the typical time-dependent variation for short (green) and long distances (orange) over 500 s. For long distances, the measured distance varied much more than in the case of a short distance on a long-term scale. This can be explained by the thermal drift of the fiber spool when simulating a long distance. As shown in Fig. 3(b), the measurement repeatability at 2 ms (without averaging) was found to be approximately 700 nm for both short and long distances. The measurement repeatability in these cases gradually improved to 200 nm with a measurement-fitted relationship of 40 nm $\times \tau_{\mathrm{avg}}^{-0.5}$, where τ_{avg} is the averaging time. For longer averaging times exceeding 0.1 s, the measurement repeatability for short distances remained at about 200 nm; however, the measurement repeatability of long distances diverged in the form of a random walk, being proportional to $\tau_{\mathrm{avg}}^{0.5}$. For a selected window of 150–180 s, the measurement repeatability can be gradually improved to 60 nm at an averaging time of 5 s.

As shown in Fig. 4, we evaluated the measurement linearity through a comparison with a commercial homodyne laser

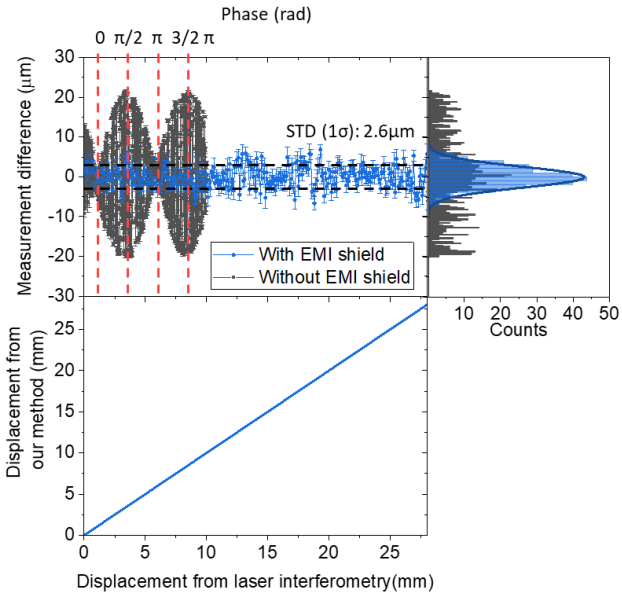

Fig. 4. Linearity test with laser displacement interferometry over 10 mm (ambiguity range) with 10 μm steps. Upper panel is measurement difference between our method and laser displacement interferometry. Gray curve shows measured periodic error without shielding for comparison. Right panel shows histogram of the residual error after shielding. Lower panel is measured displacement from our method and laser displacement interferometry.

displacement interferometer with less than 10 nm linearity error as a reference. We repeatedly measured distances over 27 mm in 10 μm steps to measure the periodic error within a single period. The measurement results showed that the measurement difference between our method of absolute distance measurement and the commercial homodyne laser displacement interferometer was ± 2.6 μm (1 σ), and there were no notable periodic patterns of measurement errors. The equivalent phase error was 1.63 mrad (0.094°), which corresponded to the phase accuracy of typical phase measurement devices. The corresponding histogram was well-fitted to a Gaussian distribution, as shown in the right panel of Fig. 4.

C. Periodic Error of the All-Fiber Photonic-Based Amplitude Modulation Distance Measurement Method

The periodic error is generally main contributor to the inaccuracy of measurement instruments and generally known to be generated by crosstalk from interferometric optics or electronic circuitry to the measurement signal [35]–[40]. This crosstalk signal is on the same frequency as the measurement signal, but its phase is independent of the target distance. Our interferometric part was well designed to minimize any back reflection beams that acted as optical crosstalk. To minimize electrical crosstalk, all microwave cables were shielded with aluminum foil. However, our goal with this configuration was an on-chip platform, where the electrical crosstalk should be considered.

As shown in Fig. 5(a) and (b), the periodic error caused by the crosstalk can be expressed as (1) and the crosstalk signal is commonly determined from the reference signal

$$A_m \cos\theta_m = A_i \cos\theta_i + \varepsilon_c \cos\theta_c. \tag{1}$$

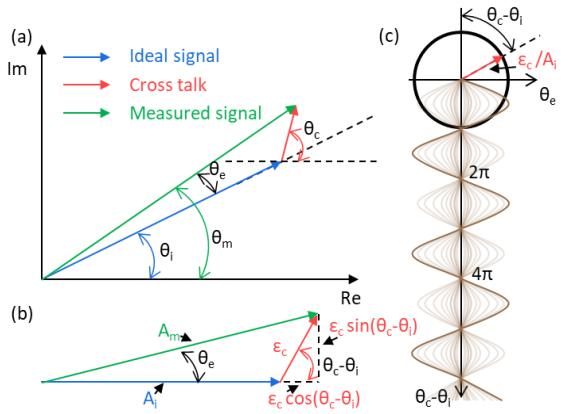

Fig. 5. Modeling of periodic error. (a) Phasor diagram for periodic error modeling. (b) Simplified phasor diagram for periodic error calculation. (c) Modeled periodic error from (3).

Here, A_m is the amplitude of the measured signal, θ_m is the measured phase, A_i is the amplitude of an ideal signal, θ_i is the ideal phase delay, ε_c is the amplitude of the crosstalk signal, and θ_c is a phase of the crosstalk signal, which is independent of the target distance. To simplify the periodic error, a phasor diagram can be used, as shown in Fig. 5(b). An analytical solution for the periodic error (θ_e) can be expressed as:

$$\tan\theta_e = \frac{\varepsilon_c \sin(\theta_c - \theta_i)}{\{A_i + \varepsilon_c \cos(\theta_c - \theta_i)\}}. \tag{2}$$

If ε_c is small enough to be negligible, (2) can be re-expressed as follows:

$$\tan\theta_e \approx \theta_e \approx \frac{\varepsilon_c \sin(\theta_c - \theta_i)}{A_i}. \tag{3}$$

From (3), the amplitude of the periodic error (θ_{e_amp}) is linearly proportional to the amplitude of the crosstalk ($\theta_{e\_amp} = \varepsilon_c / A_i$).

To observe the periodic error, we removed the aluminum jacket used as EMI shielding to artificially create electrical crosstalk. The gray line in Fig. 4 shows a typical periodic error over displacement of 10 mm, which corresponds to the ambiguity range. The minimum measurement error appeared at a measured phase close to 0 and π rad (180°), while the measurement error reached its maximum at the measured phase of nearly $\pi/2$ rad (90°) and $3/2\pi$ rad (270°). This type of periodic error is generally known to be generated by crosstalk from interferometric optics or electronic circuitry to the measurement signal [35]–[40]. The periodic error appeared as a sinusoidal pattern, which has a minimum value when $\theta_c - \theta_i$ is at 0 or π rad and a maximum value when $\theta_c - \theta_i$ is at $\pm\pi/2$ rad. If assume that the magnitude and direction of ε_c changed, the periodic error (θ_e) can be changed, as shown in Fig. 5(c). The fringe-like pattern of the periodic error, as observed here, can be explained by the random variation of the magnitude and direction of ε_c. In our measurement, the peak value of the periodic error was 20 μm, which corresponded to phase error of 12.6 mrad (0.72°). Based on (3), the amplitude ratio between an ideal signal (A_i) and the crosstalk signal (ε_c) was estimated to be 0.002, corresponding

TABLE I
UNCERTAINTY BUDGET FOR AMCW DISTANCE MEASUREMENT

Uncertainty sources	Value	Contribution
Uncertainty for modulation frequency, $u(f_{IM})$	$1.0\cdot10^{-13}$	$1.0\cdot10^{-13}\cdot L$
Uncertainty for cesium atomic clock, $u(f_{cesium})$	$1.0\cdot10^{-13}$	
Stability of RF synthesizer, $u(f_{stability})$	$4.7\cdot10^{-14}$	
Uncertainty for the refractive index air, $u(n_{air})$	$2.0\cdot10^{-7}$	$2.0\cdot10^{-7}\cdot L$
Uncertainty for Edlen equation, $u(n_{Edlen})$	$1.0\cdot10^{-8}$	
Uncertainty for air temperature, $u(n_T)$	$1.8\cdot10^{-7}$	
Uncertainty for air pressure, $u(n_P)$	$7.8\cdot10^{-8}$	
Uncertainty for humidity, $u(n_H)$	$5.8\cdot10^{-9}$	
Uncertainty for CO_2, $u(n_{CO2})$	$1.3\cdot10^{-9}$	
Uncertainty for phase detection, $u(\theta)$	$1.62\cdot10^{-3}$ rad	2.57 μm
Repeatability, $u(\theta_{repeatability})$	$5.2\cdot10^{-5}$ rad	
Long-term drift, $u(\theta_{drift})$	$2.5\cdot10^{-4}$ rad	
Phase accuracy, $u(\theta_{offset})$	$1.6\cdot10^{-3}$ rad	
Combined standard uncertainty (k=1)	$\{(2.57\ \mu m)^2+(2.0\cdot10^{-7}\cdot L)^2\}^{0.5}$	
For 0.3 m		2.57 μm
For 8 m		3.03 μm

to a PSD level of −54 dB. Even a small crosstalk signal close to noise floor can lead to significant measurement errors. This may be a critical issue in relation to the use of an integrated on-chip platform, where the electric wiring is highly dense, and highly insulating materials, which can be integrated into an on-chip platform, are required to suppress the electrical crosstalk [41].

D. Uncertainty Evaluation

Table I shows the uncertainty evaluation done to estimate the measurement performance. The uncertainty $u(L)$ of the measured distance can be categorized into three major terms as shown below

$$u(L)=\left[\{u(f_{IM})L\}^2+\{u(n_{air})L\}^2+\left\{\frac{u(\theta)}{2\pi}L_{NAR}\right\}^2\right]^{1/2}. \tag{4}$$

The first term, $u(f_{IM})$, represents the modulation frequency uncertainty of the light sources and can be expressed by the following equation:

$$u(f_{IM})=\left\{u^2(f_{Cesium})+u^2\left(f_{stability}\right)\right\}^{1/2}. \tag{5}$$

TABLE II
PERFORMANCE SUMMARY

	Repeatability	**Linearity**	**Modulation frequency**
This work	**50 nm @ 1 s**	**2.6 μm (k=1)**	**15 GHz**
[8]	N/A	44 μm (k=1)	28 GHz
[11]	N/A	50 μm (k=1)	1 GHz
[12]	N/A	10 μm (p-p value)	11.4 GHz
[14]	7 μm (k=1)	14 μm (k=1)	1 GHz
[32]	2.5 μm @ 10 s	7.8 μm (k=1)	1 GHz
[42]	N/A	60 μm (p-p value)	0.8 GHz
[43]	11 μm (k=1)	N/A	5.9 GHz
[44]	2.8 μm (k=1)	N/A	3 GHz
[45]	12 μm (k=1)	19 μm (k=1)	1 GHz
[46]	5.6 μm @ 100 s	50 μm (p-p value)	0.9 GHz
[47]	3 μm @ 400 s	9 μm (k=1)	19.5 GHz

The uncertainty of the cesium atomic clock, $u(f_{cesium})$, used for the reference frequency is 10^{-13}. The stability relative to the reference frequency of the RF synthesizer, $u(f_{stability})$, is measured by a RF heterodyning technique for high precision; it was found to be 0.69 mHz, corresponding to $4.7\cdot10^{-14}$ at a 15 GHz modulation frequency. The total contribution of the modulation frequency uncertainty is 10^{-13}. The second term, $u(n_{air})$, represents the uncertainty of the refractive index of air and can be expressed by the following equation:

$$u(n_{air})=\left\{u^2(n_{Edlen})+u^2(n_T)+u^2(n_P)+u^2(n_H)+u^2(n_{CO2})\right\}^{1/2}. \tag{6}$$

The Edlen equation was used for compensation of the refractive index of air, offering uncertainty in this case of 10^{-8}. Given the air temperature uncertainty of 0.2 K, air pressure uncertainty of 50 Pa, humidity uncertainty of 1% and carbon dioxide concentration uncertainty of 15 ppm, the refractive index of air contributed $2.0\cdot10^{-7}$ of uncertainty during the measurements under our laboratory conditions [33]. The third term, $u(\theta)$, represents the phase detection from the optical and electronic parts and can be expressed by the following equation:

$$u(\theta)=\left\{u^2\left(\theta_{repeatability}\right)+u^2(\theta_{drift})+u^2(\theta_{offset})\right\}^{1/2}. \tag{7}$$

The repeatability, long-term drift, and offset of the phase detection were calculated back to repeatability, long-term drift, and linearity of the distance measurement, respectively. The long-term drift appears to originate from the slowly varying fiber delay of the intensity modulator and was estimated from the short-distance repeatability at 100 s. Here, the offset

included the effects of heterodyned signal distortion, the amplitude-to-phase conversion, and back reflection in both the optical and electrical paths. The repeatability, long-term drift, and offset of the phase detection contributed $5.2 \cdot 10^{-5}$, $2.5 \cdot 10^{-4}$, and $1.6 \cdot 10^{-3}$ rad, respectively. The uncertainty of the phase detection was estimated to be 2.57 μm; these values are not affected by an increase in L and are mainly limited by the phase offset. The combined standard uncertainty ($k = 1$) of the measured distance was evaluated to $u(L) = \{(2.57\ \mu\text{m})^2 + (2.0 \cdot 10^{-7} \cdot L)^2\}^{0.5}$. For example, the combined standard uncertainties were corresponded to 2.57 and 3.03 μm for 0.3 and 8 m, respectively.

IV. Conclusion and Perspectives

In summary, we evaluated the measurement accuracy of an all-fiber photonic microwave modulation-based absolute distance measurement method, of which the repeatability was evaluated based on our previous study. Our configuration as described in this study has direct traceability to the length standard of a cesium atomic clock with frequency uncertainty of 10^{-13}. The measurement linearity was mainly limited for two reasons: the amplitude-to-phase conversion and the periodic error. In our previous work [4], we resolved the amplitude-to-phase conversion issue, which can cause measurement linearity errors of hundreds of micrometers during the electronics-based microwave frequency down-conversion process [32], by means of photonic-microwave-mixing-based microwave frequency down-conversion. Here, we evaluated the measurement linearity of our method. We found that our method has measurement linearity error of ± 2.6 μm ($1\ \sigma$) over 27 mm, with notable periodic error levels not observed. In addition, the periodic error was theoretically derived and experimentally verified by adding an artificial electrical crosstalk signal.

Table II summarizes the measurement repeatability and linearity with a comparison with a state-of-the-art amplitude modulated continuous wave (AMCW) distance-measurement system. Because our system has a simple and all-fiber structure and excellent measurement performance, as shown in Table II, we believe that the configuration proposed here can be used in real world and not merely in laboratories, and it can be fabricated on fully integrated photonic chips with the help of silicon photonics, which will be a powerful tool in the era of the fourth industrial revolution.

References

[1] Z. Tang, Y. Li, J. Yao, and S. Pan, "Photonics-based microwave frequency mixing: Methodology and applications," *Laser Photon. Rev.*, vol. 14, no. 1, Jan. 2020, Art. no. 1800350.

[2] G. Li, "Recent advances in coherent optical communications," *Adv. Opt. Photon.*, vol. 1, no. 2, pp. 279–307, Feb. 2009.

[3] R. Schmogrow, "Error vector magnitude as a performance measure for advanced modulation formats," *IEEE Photon. Technol. Lett.*, vol. 24, no. 1, pp. 61–63, Jan. 1, 2012.

[4] Y.-S. Jang, J. Park, and J. Jin, "Sub 100-nm precision distance measurement by means of all-fiber photonic microwave mixing," *Opt. Exp.*, vol. 29, no. 8, pp. 12229–12239, Apr. 2021.

[5] N. Bobroff, "Recent advances in displacement measuring interferometry," *Meas. Sci. Technol.*, vol. 4, no. 9, pp. 907–926, Sep. 1993.

[6] J. Jin, "Dimensional metrology using the optical comb of a mode-locked laser," *Meas. Sci. Technol.*, vol. 27, no. 2, Feb. 2016, Art. no. 022001.

[7] Y.-S. Jang and S.-W. Kim, "Distance measurements using mode-locked lasers: A review," *Nanomanuf. Metrol.*, vol. 1, no. 3, pp. 131–147, 2018.

[8] J. Lee, Y.-J. Kim, K. Lee, S. Lee, and S.-W. Kim, "Time-of-flight measurement using femtosecond light pulses," *Nature Photon.*, vol. 4, no. 10, pp. 716–720, Aug. 2010.

[9] Y. Na *et al.*, "Ultrafast, sub-nanometre-precision and multifunctional time-of-flight detection," *Nature Photon.*, vol. 14, no. 6, pp. 355–360, Feb. 2020.

[10] I. Fujima, S. Iwasaki, and K. Seta, "High-resolution distance meter using optical intensity modulation at 28 GHz," *Meas. Sci. Technol.*, vol. 9, no. 7, pp. 1049–1052, Jul. 1998.

[11] K. Minoshima and H. Matsumoto, "High-accuracy measurement of 240-m distance in an optical tunnel by use of a compact femtosecond laser," *Appl. Opt.*, vol. 39, no. 30, pp. 5512–5517, 2000.

[12] N. R. Doloca, K. Meiners-Hagen, M. Wedde, F. Pollinger, and A. Abou-Zeid, "Absolute distance measurement system using a femtosecond laser as a modulator," *Meas. Sci. Technol.*, vol. 21, no. 11, Nov. 2010, Art. no. 115302.

[13] Y.-S. Jang, K. Lee, S. Han, J. Lee, Y.-J. Kim, and S.-W. Kim, "Absolute distance measurement with extension of nonambiguity range using the frequency comb of a femtosecond laser," *Opt. Eng.*, vol. 53, no. 12, Dec. 2014, Art. no. 122403.

[14] Y.-S. Jang, W. Kim, H. Jang, and S.-W. Kim, "Absolute distance meter operating on a free-running mode-locked laser for space mission," *Int. J. Precis. Eng. Manuf.*, vol. 19, no. 7, pp. 975–981, Aug. 2018.

[15] J. Dale, B. Hughes, A. J. Lancaster, A. J. Lewis, A. J. Reichold, and M. S. Warden, "Multi-channel absolute distance measurement system with sub ppm-accuracy and 20 m range using frequency scanning interferometry and gas absorption cells," *Opt. Exp.*, vol. 22, no. 20, pp. 24869–24893, 2014.

[16] E. Baumann, F. R. Giorgetta, J.-D. Deschenes, W. C. Swann, I. Coddington, and N. R. Newbury, "Comb-calibrated laser ranging for three-dimensional surface profiling with micrometer- level precision at a distance," *Opt. Exp.*, vol. 22, no. 21, pp. 24914–24928, Oct. 2014.

[17] H. Pan, X. Qu, and F. Zhang, "Micron-precision measurement using a combined frequency-modulated continuous wave ladar autofocusing system at 60 meters standoff distance," *Opt. Exp.*, vol. 26, no. 12, pp. 15186–15198, May 2018.

[18] K.-N. Joo and S.-W. Kim, "Absolute distance measurement by dispersive interferometry using a femtosecond pulse laser," *Opt. Exp.*, vol. 14, no. 13, pp. 5954–5960, 2006.

[19] S. A. van den Berg, S. T. Persijn, G. J. P. Kok, M. G. Zeitouny, and N. Bhattacharya, "Many-wavelength interferometry with thousands of lasers for absolute distance measurement," *Phys. Rev. Lett.*, vol. 108, no. 18, May 2012, Art. no. 183901.

[20] J. Park, J. Jin, J.-A. Kim, and J. Kim, "Absolute distance measurement method without a non-measurable range and directional ambiguity based on the spectral-domain interferometer using the optical comb of the femtosecond pulse laser," *Appl. Phys. Lett.*, vol. 109, no. 24, pp. 1–5, Dec. 2016.

[21] J. Jin, Y.-J. Kim, Y. Kim, S.-W. Kim, and C.-S. Kang, "Absolute length calibration of gauge blocks using optical comb of a femtosecond pulse laser," *Opt. Exp.*, vol. 14, no. 13, pp. 5974–5986, Jun. 2006.

[22] G. Wang *et al.*, "Absolute positioning by multi-wavelength interferometry referenced to the frequency comb of a femtosecond laser," *Opt. Exp.*, vol. 23, no. 7, pp. 9121–9129, Apr. 2015.

[23] Y.-S. Jang *et al.*, "Comb-referenced laser distance interferometer for industrial nanotechnology," *Sci. Rep.*, vol. 6, no. 1, Aug. 2016, Art. no. 31770.

[24] I. Coddington, W. C. Swann, L. Nenadovic, and N. R. Newbury, "Rapid and precise absolute distance measurements at long range," *Nature Photon.*, vol. 3, pp. 351–356, May 2009.

[25] H. Zhang, H. Wei, X. Wu, H. Yang, and Y. Li, "Absolute distance measurement by dual-comb nonlinear asynchronous optical sampling," *Opt. Exp.*, vol. 22, no. 6, pp. 6597–6604, 2014.

[26] Z. Zhu, G. Xu, K. Ni, Q. Zhou, and G. Wu, "Synthetic-wavelength-based dual-comb interferometry for fast and precise absolute distance measurement," *Opt. Exp.*, vol. 26, no. 5, pp. 5747–5757, Feb. 2018.

[27] M.-G. Suh and K. J. Vahala, "Soliton microcomb range measurement," *Science*, vol. 359, no. 6378, pp. 884–887, Feb. 2018.

[28] J. Riemensberger *et al.*, "Massively parallel coherent laser ranging using a soliton microcomb," *Nature*, vol. 581, no. 7807, pp. 164–170, May 2020.

[29] Y.-S. Jang, H. Liu, J. Yang, M. Yu, D.-L. Kwong, and C. W. Wong, "Nanometric precision distance metrology via hybrid spectrally resolved and homodyne interferometry in a single soliton frequency microcomb," *Phys. Rev. Lett.*, vol. 126, no. 2, Jan. 2021, Art. no. 023903.
[30] S. H. Lee *et al.*, "Accuracy evaluation of an optically pumped caesium beam frequency standard KRISS-1," *Metrologia*, vol. 46, no. 3, pp. 227–236, Mar. 2009.
[31] B. Schwarz, "Mapping the world in 3D," *Nature Photon.*, vol. 4, pp. 429–430, Jul. 2010.
[32] W. Kim, H. Fu, K. Lee, S. Han, Y.-S. Jang, and S.-W. Kim, "Photonic microwave distance interferometry using a mode-locked laser with systematic error correction," *Appl. Sci.*, vol. 10, no. 21, p. 7649, Oct. 2020.
[33] Y.-S. Jang and S.-W. Kim, "Compensation of the refractive index of air in laser interferometer for distance measurement: A review," *Int. J. Precis. Eng. Manuf.*, vol. 18, no. 12, pp. 1881–1890, Dec. 2017.
[34] J. Guillory, J. García-Márquez, C. Alexandre, D. Truong, and J.-P. Wallerand, "Characterization and reduction of the amplitude-to-phase conversion effects in telemetry," *Meas. Sci. Technol.*, vol. 26, no. 8, Aug. 2015, Art. no. 084006.
[35] H. Kikuta, K. Iwata, and R. Nagata, "Absolute distance measurement by wavelength shift interferometry with a laser diode: Some systematic error sources," *Appl. Opt.*, vol. 26, no. 9, pp. 1654–1660, May 1987.
[36] T. Eom, T. Choi, K. Lee, H. Choi, and S. Lee, "A simple method for the compensation of the nonlinearity in the heterodyne interferometer," *Meas. Sci. Technol.*, vol. 13, no. 2, pp. 222–225, Feb. 2002.
[37] K. Minoshima, T. R. Schibli, and H. Matsumoto, "Study on cyclic errors in a distance measurement using a frequency comb generated by a mode-locked laser," in *Proc. CLEO*, San Francisco, CA, USA, May 2004, pp. 1–2.
[38] K.-N. Joo, J. D. Ellis, E. S. Buice, J. W. Spronck, and R. H. M. Schmidt, "High resolution heterodyne interferometer without detectable periodic nonlinearity," *Opt. Exp.*, vol. 18, no. 2, pp. 1159–1165, Jan. 2010.
[39] H. Fu, P. Hu, J. Tan, and Z. Fan, "Nonlinear errors induced by intermodulation in heterodyne laser interferometers," *Opt. Lett.*, vol. 42, no. 3, pp. 427–430, Jan. 2017.
[40] S. Yokoyama, Y. Hori, T. Yokoyama, and A. Hirai, "A heterodyne interferometer constructed in an integrated optics and its metrological evaluation of a picometre-order periodic error," *Precis. Eng.*, vol. 54, pp. 206–211, Oct. 2018.
[41] A. Iqbal *et al.*, "Anomalous absorption of electromagnetic waves by 2D transition metal carbonitride Ti_3CNT_x (MXene)," *Science*, vol. 369, no. 6502, pp. 446–450, Jul. 2020.
[42] H. Yang, P. Hu, and J. Tan, "Long-distance measurement applying two high-stability and synchronous wavelengths," *IEEE Trans. Instrum. Meas.*, vol. 64, no. 3, pp. 750–757, Mar. 2015.
[43] J. Guillory, R. Smíd, J. García-Márquez, D. Truong, C. Alexandre, and J.-P. Wallerand, "High resolution kilometric range optical telemetry in air by radio frequency phase measurement," *Rev. Sci. Instrum.*, vol. 87, no. 7, Jul. 2016, Art. no. 075105.
[44] A. Kadambi and R. Raskar, "Rethinking machine vision time of flight with GHz heterodyning," *IEEE Access*, vol. 5, pp. 26211–26223, 2017.
[45] D. Salido-Monzu, "Simultaneous distance measurement at multiple wavelengths using the intermode beats from a femtosecond laser coherent supercontinuum," *Opt. Eng.*, vol. 57, no. 4, p. 1, Apr. 2018.
[46] X. Xu *et al.*, "Long distance measurement by dynamic optical frequency comb," *Opt. Exp.*, vol. 28, no. 4, pp. 4398–4411, Feb. 2020.
[47] L.-Y. Chen, A. K. Vinod, J. Mcmillan, C. W. Wong, and C.-K.-K. Yang, "A 9-μm precision 5-MSa/s pulsed-coherent LiDAR system with subsampling receiver," *IEEE Solid-State Circuits Lett.*, vol. 3, pp. 262–265, 2020.

Yoon-Soo Jang received the Ph.D. degree in mechanical engineering from the Korea Advanced Institute of Science and Technology, Daejeon, Republic of Korea, in 2017.

From 2018 to 2019, he was a Post-Doctoral Research Scientist with Mesoscopic Optics and Quantum Electronics Laboratory, UCLA, Los Angeles, CA, USA. He is currently a Senior Research Scientist with the Korea Research Institute of Standards and Science, Daejeon. His research interests include optical metrology, ultrafast photonics, mode-locked laser, frequency comb, and laser interferometry.

Jungjae Park received the Ph.D. degree in mechanical engineering from the Korea Advanced Institute of Science and Technology, Daejeon, Republic of Korea, in 2009.

From 2010 to 2011, he was a Post-Doctoral Research Scientist with Surface and Microform Metrology Group, NIST, Gaithersburg, MD, USA. He is currently a Principal Research Scientist with the Korea Research Institute of Standards and Science, Daejeon, and a Professor with the Department of Science of Measurement, University of Science and Technology, Daejeon. His research interest includes optical metrology.

Jonghan Jin received the Ph.D. degree in mechanical engineering from the Korea Advanced Institute of Science and Technology, Daejeon, Republic of Korea, in 2006.

From 2006 to 2008, he was a Post-Doctoral Research Scientist with mechanical engineering, KAIST, Daejeon. He is currently a Principal Research Scientist with the Korea Research Institute of Standards and Science, Daejeon, and a Chief Major Professor with the Department of Science of Measurement, University of Science and Technology, Daejeon. His research interests include optical interferometry, optical comb-based length metrology, and AI-metrology.